Chapter 1. Global agroclimatic patterns

Chapter 1 describes the CropWatch agroclimatic indicators for rainfall (RAIN), temperature (TEMP), and radiation (RADPAR), along with the agronomic indicator for potential biomass (BIOMSS) for sixty-five global Monitoring and Reporting Units (MRU). Rainfall, temperature, and radiation indicators are compared to their average value for the same period over the last fourteen years (called the "average"), while BIOMSS is compared to the indicator's average of the recent five years. Indicator values for all MRUs are included in Annex A, table A.1. For more information about the MRUs and indicators, please see Annex C and online CropWatch resources at www.cropwatch.com.cn.

1.1 Overview

Global patterns of rainfall for the four-month monitoring period of July to October 2015 are largely compatible with El Niño impacts, with several marked and regionally well-defined anomalies, especially in Central and South America, east and southern Africa as well as Southeast Asia and Oceania.

However, as is increasingly noted by the climate monitoring community, there is no such thing as a "normal" El Niño, nor is there any typical and predictable behaviour when moving beyond very broad regional patterns. El Niño means havoc, i.e. droughts, floods and cyclones, but the details change every time. For instance, the classical pattern would mean wet conditions in the Horn of Africa and east Africa, and drought in the south, as happened in 1991-1992.

During the current season, we have dry conditions over all of south and east Africa for the reporting period, with more severe impacts in the east as the CropWatch RAIN index shows a deficit of 19% in southern Africa (Mapping and Reporting Unit, MRU-09), and as much as 25% and 28% in the Horn of Africa (MRU-04) and the eastern African Highlands (MRU-02), respectively. Even equatorial central Africa (MRU-01) is affected (-6%) and north and central Madagascar (MRU-05) recorded above average RAIN (+12%).

Throughout the Caribbean, Central and South America suffered from drought (with deficits between 20% and 30%), except the east, from the Brazilian Nordeste (MRU-22) to the Argentinian Pampas (MRU-26), where the excess reached 53% in central-eastern Brazil (MRU-23).

As described in subsequent sections of this chapter, there are also spatially coherent patterns of abnormal rainfall in western, central and eastern Asia. They are, however, not part of the "normal" El Niño impacts, which stresses again that the currently on-going El Niño is rather atypical, except maybe in Oceania.

An unusually weak association between the climate variables also characterizes the current reporting period. For instance, there is no discernible link between rainfall and temperature anomalies, at the global or even regional scales, including latitudinal variations. The loose association between RAIN and the CropWatch radiation indicator (RADPAR) is negative during the reporting period, as expected, but not statistically significant.

With the exception of Subarctic America (MRU-65) of which only the extreme south holds some agricultural relevance, all other extremes do not follow any pattern (table 1.1).

Table 1.1. RAIN, TEMP and RADPAR anomalies in the global MRU with the largest rain anomalies

MRU	RAIN (%)	TEMP (°C)	RADPAR (%)
56. New Zealand	-73	-0.5	-4
53. Northern Australia	-71	-0.7	5
65. Subarctic America	165	1.9	-8
32. Gansu-Xinjiang (China)	173	-0.4	0
47. Mongolia region	309	-0.1	0

Not all impacts of El Niño will be negative. For instance, the aforementioned rainfall anomaly of -6% in equatorial central Africa (MRU-01) is accompanied by a drop in temperature (-0.7°C) and an increase in sunshine (+6%), which corresponds to favourable conditions: The areas have abundant rainfall largely exceeding crop water requirements, low sunshine is usually limiting crop growth and night-time respiration loss is significant due to high temperature. Similar situations can only be identified on a case-by-case basis due to the absence of coherent spatial patterns among the climate variables.

1.2 Rainfall

During the monitoring period, lower-than-average rainfall occurred in many regions around the world as can be seen on figure 1.1.

Abnormal rainfall deficits occurred in some major agricultural areas of Asia, including Punjab to Gujarat (MRU-48, -41%), East Asia (MRU-43, -48%), Huanghuaihai in China (MRU-34, -30%), northeast China (MRU-38, +24%), Hainan (MRU-33, -41%), Taiwan (MRU-42, -25%) and maritime Southeast Asia (MRU-49, -52%).

Unfortunately, drought continued in major production zones in Australia, Europe and Africa, including New Zealand (MRU-56 -73%), Queensland to Victoria (MRU-54, -43%), north Australia (MRU-53, -71%), Ukraine to the Ural Mountains (MRU-58, -25%) and non-Mediterranean Western Europe (MRU-60, -16%).

With the exception of north African Mediterranean areas (MRU-07, +46%), below average rainfall prevailed in Africa, including the East African highlands (MRU-02, -28%), the Horn of Africa (MRU-04, -25%), southern Africa (MRU-09, -19%) and Western Cape in South Africa (MRU-10, -19%).

Above average rainfall occurred in major production zones in both North and South America, including the Pampas (MRU-26, +35%), Central eastern Brazil (MRU-23, +53%), and the Northern Great Plains (MRU-12, +45%). Abundant rainfall fell over some pastoral regions, including Southern Mongolia (MRU-47, +309%), Gansu-Xinjiang (MRU-32, +173%) and the Ural to Altai Mountains (MRU-62, +50%).

Figure 1.1. Global map of rainfall anomaly (as indicated by the RAIN indicator) by MRU, departure from 14YA, July-October 2015 (percentage)

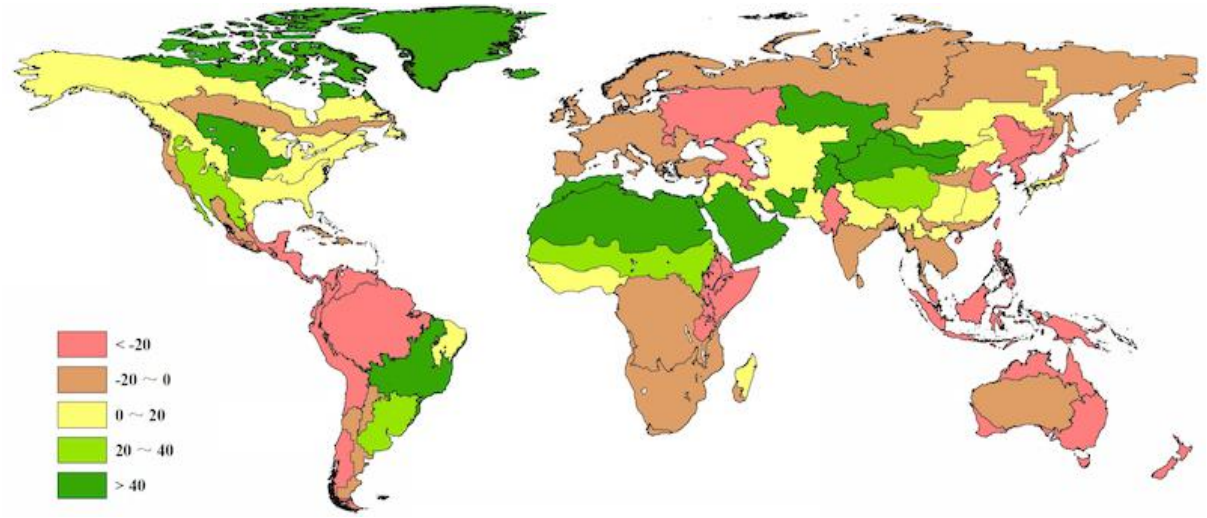

Note: Data for July-October, compared with the fourteen-year average (14YA) for the same period 2001-2014.

1.3 Temperature

Over the reporting period, the temperature departures of different MRUs show different patterns across continents (figure 1.2). In Eurasia, most MRUs show a negative departure compared to the average. The temperatures in the region from the Ural to the Altai Mountains, the Lower Yangtze (China) and southern Japan and Korea (MRU-62, -1.1°C, MRU-37, -1.3°C and MRU-46, -1.2°C respectively) were significantly below average by more than 1°C. Only in Mediterranean Europe and Turkey, Caucasus, eastern Central Asia and eastern Siberia (MRU-59, 0.9°C; MRU-29, 0.6°C; MRU-52, 1.0°C and MRU-51, 0.1°C respectively), were temperature departures positive.

In North America, the temperature was close to average except on the West Coast (MRU-16), with a departure of 0.9°C. In northern South America, the temperature departures were positive but negative in the Southern Cone, especially in central-north Argentina, western Patagonia and the semi-arid Southern Cone (MRU-25, -0.6°C; MRU-27, -0.5°C and MRU-28, -0.8°C respectively), where the temperature was below average by more than 0.5°C.

In Africa and Australia, the greatest negative temperature departures are found in south-western Madagascar (MRU-06, -1.1°C). In most other areas, the temperature was close to average and the departures were less than 1°C.

Figure 1.2. Global map of air temperature anomaly (as indicated by the TEMP indicator) by MRU, departure from 14YA, July-October 2015 (degrees Celsius)

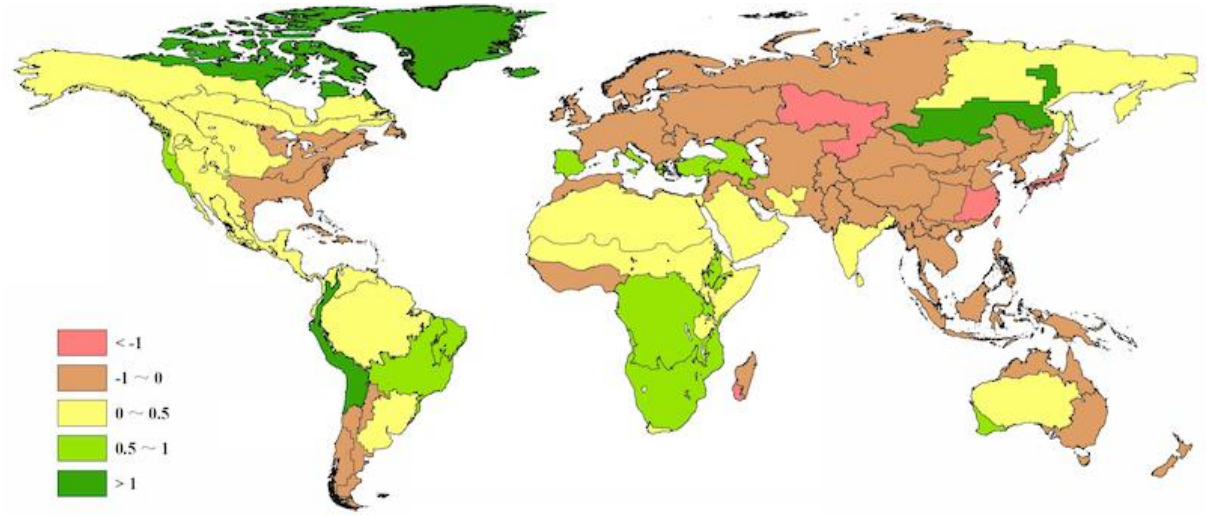

Note: Data for July-October 2015, compared with the fourteen-year average (14YA) for the same period 2001-2014.

1.4 Photosynthetically active radiation

As a key agroclimatic indicator, Photosynthetically Active Radiation (PAR, as assessed by the CropWatch agroclimatic indicator RADPAR) has an obvious relationship with temperature and rainfall patterns: abundant rainfall is associated with high cloudiness, which leads to low daytime temperatures, mostly in temperate areas. Compared to the recent average of the total 65 MRUs, slightly more than half of them are above average (figure 1.3).

The highest departure from the recent reference period occurred in central north Argentina (MRU-25) and the Pampas (MRU-26), with 10% and 9% decrease in PAR respectively. RADPAR also shows a decrease in the northernmost area of the continent, which is not of agricultural relevance, Sub Arctic America (MRU-65) where the variable dropped 8%, and Boreal North America (MRU-61) where it decreased by 3% compared to the average.

Record high PAR departures are concentrated in several adjacent areas, including (i) East African Highlands (MRU-02, +7%), equatorial central Africa (MRU-01, +6%) and the Horn of Africa (MRU-04, +4%); (ii) the Caribbean (MRU-20, +5%) and Amazon (MRU-24, +5%); (iii) Southeast Asia islands (MRU-49, +9%) and Southern Asia (MRU-45, +6%).

In China, the major paddy rice production areas, the Lower Yangtze (MRU-37) and southern China (MRU-40), show significant a decrease in terms of PAR with -8% and -7% respectively. South-west China (MRU-41) also experienced below average PAR with a -3% departure, which probably results from the cloudiness associated with abundant rainfall in the region. The areas with high PAR are the Chinese Loess Region (MRU-36, +7%), Huanghuaihai (MRU-34, +5%), and Hainan (MRU-33, +3%). The rest of China generally shows average PAR level during the current reporting period.

Figure 1.3. Global map of PAR anomaly (as indicated by the RADPAR indicator) by MRU, departure from 14YA July-October 2015 (percentage)

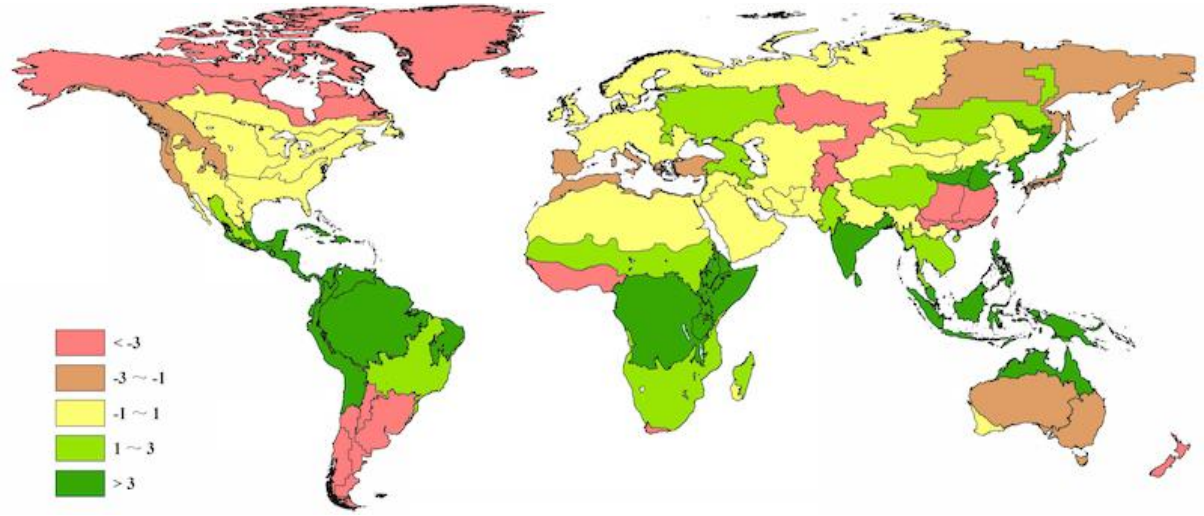

Note: Data for July-October 2015, compared with the fourteen-year average (14YA) for the same period 2001-2014.

1.5 Biomass

BIOMSS is a synthetic agro-climatic indicator that takes into account rainfall and temperature to estimate the potential biomass accumulation. Recent departures from average for the 65 global MRUs are shown in figure 1.4.

During this monitoring period, the notable change in rainfall compared with the average has affected the biomass production potential across the world. Over the reporting period, biomass variations are brought about more by RAIN anomalies than by TEMP anomalies (the R-squared between BIOMSS and RAIN and between BIOMSS and TEMP are 0.83 and 0.07 respectively).

Due to favorable rainfall in Eurasia, Africa and America, the BIOMSS in 28 MRUs show an upward trend compared with the average of the last five years. The greatest positive BIOMSS departures are found in the Northern Great Plains (MRU-12, 45% on RAIN and 30% on BIOMSS), the southwest United States and north Mexican highlands (MRU-18, 33% on RAIN and 36% on BIOMSS), North Africa-Mediterranean (MRU-07, 46% on RAIN and 36% on BIOMSS), central eastern Brazil (MRU-23, 53% on RAIN and 38% on BIOMSS), Ural to Altai mountains (MRU-62, 50% on RAIN and 39% on BIOMSS), Gansu-Xinjiang (China) (MRU-32, 173% on RAIN and 90% on BIOMASS), and southern Mongolia (MRU-47, 309% on RAIN and 125% on BIOMSS).

Declines in BIOMSS (compared to average values for the same period) are similarly affected by significantly decreased rainfall: In the following MRUs, the BIOMSS departures are well below the average of the last five years: Northern Australia (MRU-53, -71% on RAIN and -71% on BIOMSS), New Zealand (MRU-56, -73% on RAIN and -60% on BIOMSS), maritime Southeast Asia (MRU-49, -52% on RAIN and -47% on BIOMSS), Queensland to Victoria (MRU-54, -43% on RAIN and -43% on BIOMSS), Punjab to Gujarat (MRU-48, -41% on RAIN and -43% on BIOMSS) and East Asia (MRU-43, -48% on RAIN and -30% on BIOMSS).

Figure 1.4. Global map of biomass accumulation (BIOMSS) by MRU, departure from 5YA, July-October (percentage)

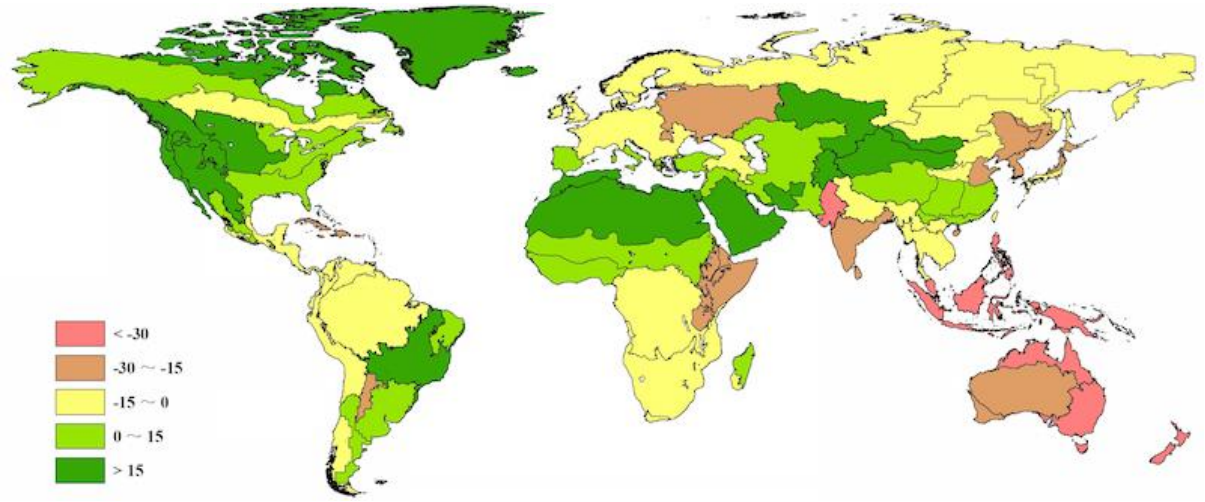

Note: Data for July-October 2015, compared with the five-year average (5YA) for the same period 2010-2014.